Article

Adsorption of Eosin B from Wastewater onto the Prepared Porous Anion Exchange Membrane

Muhammad Imran Khan, Noureddine Elboughdiri,* Abdallah Shanableh, Asma Manzoor, Suryyia Manzoor, Nosheen Farooq, Jannat Suleman, Hadia Sarwar, Mhamed Benaissa, and Yacine Benguerba

Read Online

ACCESS | Metrics & More | Article Recommendations | SI Supporting Information

ABSTRACT: This research describes the fabrication of the porous trimethylamine (TMA)-grafted anion exchange membrane (AEM) over a phase inversion process. The synthesis of the generated AEM was verified using Fourier transform infrared (FTIR) spectroscopy. The fabricated porous AEM showed 240% water uptake (W_R), 1.45 mg/g ion exchange capacity (IEC), and a 9.0% linear expansion ratio (LER) at 25 °C. It exhibited a porous structure and higher thermal stability. It was utilized to remove eosin B (EB) from wastewater via the process of adsorption. The adsorption capacity of EB increased with time and the starting concentration of EB while decreasing with temperature and the AEM dosage. Adsorption isotherm investigation results showed that EB adsorption onto the porous AEM followed the Langmuir isotherm because the value of correlation coefficient ($R^2 = 0.992$) was close to unity. Because the correlation coefficient was close to one, it was determined through adsorption kinetic experiments that the adsorption of EB on the produced porous AEM was suitable for a pseudo-second-order model. Thermodynamic study about process of EB adsorption on the porous AEM revealed that there was an exothermic ($\Delta H° = -16.60$ kJ/mol) and spontaneous process.
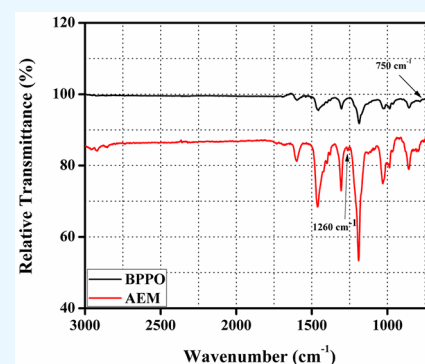
1. INTRODUCTION

Dyes make up a class of chemical molecules that give other things their vibrant, solid color. Benzene, naphthalene, anthracene, xylene, and other aromatic hydrocarbons are commonly utilized to create the complex aromatic molecular structures found in synthetic colors.[1] Dyes, which are frequently employed in the plastic, paper, textile, food, and cosmetic industries, are readily recognizable pollutants.[2] Decolorizing clothing and creating wastewater are new problems in environmental management.[3] Dyes may significantly affect the photosynthetic activities of aquatic life since they contain hazardous elements including aromatic metals, chlorides, and several other poisons.[4] Numerous industrial colors are resistant to light, aerobic digestion, and oxidation,[5] while dyes are typically derived from artificial sources and have an aromatic chemical structure that increases their durability. As a result, it is difficult to handle these contaminants, since they are neither biodegradable nor photodegradable.[6] Therefore, dye removal from industrial effluents is a key requirement.

For dye removal, a variety of methods have been utilized up to this point, including sophisticated oxidation techniques, coagulation and flocculation, electro-oxidation, and ultra-filtration. In addition to coagulation or flocculation, biological degradation, separation processes, and reverse osmosis, several techniques were used for the removal of colorants and the management of wastewater. These included electrodialysis,

filtering, and flotation.[7−17] The large use of chemical reagents and electrical energy in these procedures is a common problem.[10] Adsorption is considered a basic approach for treating wastewater due to its simplicity and low cost.[18−21] An excellent alternative for the treatment of wastewater is provided if an adsorbent is effective and does not require any additional preparation steps before use.[22,23] Additionally, this method is an environmentally friendly option because it functions at standard pressure and temperature while simultaneously releasing dyes.[19] The acceptability of utilizing a variety of adsorbents with variable costs and efficacies has already been studied by researchers, such as waste apricot,[24] shells of coconuts,[25] dairy waste,[26] treated bamboo grass, modified peat—resin particles,[27] citrus peels,[28] nut hulls,[1] the shell of a pistachio nut,[29] husks of rice,[30] bagasse and powdered nut shell charcoal,[31] bamboo,[32] jackfruit peels,[33] palm tree trash, and date stones,[34] for dye and heavy metal wastewater discharge.

Currently, the interaction between the adsorbate and the functional groups of the adsorbents determines the efficacy of all adsorbents used for the discharge of dyes and heavy metal ions.[35] A membrane's ability to adsorb pollutants and release them from wastewater depends on the quantity of adsorption sites and the surface area of the matrix.[36−38] The anion exchange membrane (AEM) may thus be considered an acceptable substitute due to its substantial adsorption surface area for dye discharge from aqueous solutions. P81 and ICE450 membranes were used to remove methyl violet 2B from an aqueous solution by adsorptive removal.[39] Additionally, an aqueous solution of cibacron blue 3GA was eliminated utilizing AEMs.[40] In the past, we discussed how to remove dyes using a variety of produced and commercial AEMs from wastewater.[23,41−44] In this Article, we shall develop the porous trimethylamine (TMA)-grafted AEM for eosin B (EB) removal from effluent. According to what we know, no published study on the use of a porous trimethylamine (TMA)-grafted AEM for EB adsorption from wastewater is accessible in the literature. In addition, EB is an anion dye. It possesses negatively charged ions in an aqueous solution. The prepared porous AEM (adsorbent) exhibited a positive charge. There will be a force of attraction between the positively charged AEM surfaces and negatively charged dye molecules in the dye solution. For this reason, we selected EB as a pollutant in this research.

This research focuses on the fabrication of a porous TMA-grafted AEM via the phase inversion method. The developed porous AEM's ion exchange capability, structure, linear expansion ratio, thermal stability, and water absorption were all examined. To demonstrate the effective synthesis of the porous AEM, we used FTIR spectroscopy. The developed porous AEM was utilized to remove EB from wastewater via an adsorption process. The dependence of EB adsorption on the porous AEM mass, contact duration, temperature, and EB initial concentration in solution was investigated in detail. EB adsorption on porous AEM was also studied regarding kinetics, equilibrium, and thermodynamics.

2. EXPERIMENTAL SECTION

2.1. Materials. Sinopharm Chemical Reagent Co. Ltd. provided eosin B, potassium chromate, silver nitrate, N-methyl-2-pyrrolidone, sodium chloride, and trimethylamine. They were used for manipulation by intended means. For the duration of this study, distilled water was used. The brominated poly(2, 6-dimethyl-1,4-phenyleneoxide) (BPPO) was supplied by Tianwei Membrane Co. Ltd. of Shandong province in China.

2.2. Porous AEM Fabrication. We fabricated the porous AEM by adding TMA into a BPPO matrix using the phase inversion approach as described in our prior work.[45−47] 3.0 g of BPPO was first dissolved in N-methyl-2-pyrrolidone (NMP) to produce the 30% solution. A measured volume of TMA was combined with the produced BPPO solution (0.30 g). The mixture of components was continuously stirred at 40 °C throughout the night to speed up the reaction between trimethylamine and BPPO. The mixture was then transferred to a transparent tray and immediately immersed in ethanol. The membranes were washed by soaking them in water for 2 days. Figure S1 depicts the chemical structure of the ready porous AEM.

2.3. Characterizations. *2.3.1. Instrumentation.* The production of porous AEMs was confirmed using an FTIR

spectrometer (Vector 22, Bruker) that used attenuated total reflectance (ATR) in the 4000−400 cm^{-1} range. A Shimadzu TGA-50H analyzer was used to look at thermal stability across a temperature range of 25−800 °C with a heating rate of 10 °C/min under nitrogen flow. The morphology was examined by field emission scanning electron microscopy (FE-SEM, Sirion200, FEI Company, USA).

2.3.2. Ion Exchange Capacity, Linear Swelling Ratio, and Water Uptake. The created porous AEM's water absorption was examined as indicated.[48−52] An AEM that had been dried and precisely weighed was submerged in distilled water at 25 °C. After using tissue paper to wipe away the surface water, the AEM's wet weight was determined. The mass difference between the dried and undried porous AEM was used to estimate water absorption using the following formula:

$$W_R = \frac{W_{WET} - W_{DRY}}{W_{DRY}} \times 100\% \tag{1}$$

The wet and dry masses of AEMs are represented by W_{WET} and W_{DRY}, respectively.

A prepared porous AEM was cut into 4×4 cm^2 pieces in order to evaluate the porous AEM's linear swelling ratio (LSR) at 25 °C. The LSR was measured using the equation below, which was calculated:[53,54]

$$LER = \frac{(L_{WET} - L_{DRY})}{L_{DRY}} \times 100\% \tag{2}$$

The lengths of the membrane samples are shown in eq 2 as L_{WET} and L_{DRY}, respectively, for the wet and dry forms.

The capacity for ion exchange was recorded using the classical Mohr's procedure as reported in previous work.[55,56] A 1.0 M NaCl solution was used to soak the measured mass of the dry porous AEM for 2 days to convert all charge sites to the Cl$^-$ form. The porous AEM was rinsed in deionized water to remove excessive NaCl before being immersed in a 0.5 M Na$_2$SO$_4$ solution for 2 days. By employing K$_2$CrO$_4$ as an indicator and titrating with 0.05 M AgNO$_3$, we calculated the weight of the released Cl$^-$ ions. The following equation was used to determine the ion exchange capacity (IEC):

$$IEC = \frac{C_{AgNO_3} V_{AgNO_3}}{W_{DRY}} \tag{3}$$

where W, V, and C indicate the dried membrane's weight, the volume of AgNO$_3$ used during titration, and the concentration of the AgNO$_3$ solution, respectively.

2.4. EB Adsorption on the Porous AEM. The adsorption of EB on the developed porous AEM was conducted as described.[19,55,57−61] To determine the ideal contact time, the small pieces of the developed porous AEM containing a measured mass (0.1 g) had been shaken for 50, 100, 200, 300, 400, 500, 900, 1200, and 1400 min in 40 mL of EB solution with a 50 mg/L starting concentration. Using its various masses of 0.02, 0.04, 0.06, 0.08, and 0.10 g in 40 mL of EB solution with an EB starting concentration of 50 mg/L for 1440 min, we discovered the optimal mass of the piece of porous AEM. To investigate isotherms of adsorption, the computed mass of the pieces of porous AEM (0.10 g) were shaken for 1440 min into 40 mL of EB solution starting with 50, 100, 200, 300, 400, 500, 800, and 1000 mg/L concentrations. To conduct an adsorption thermodynamics investigation, the measured masses of a piece of the porous AEM (0.1 g) were then stirred at 200 rpm into 40 mL of EB

solution with an initial concentration of 50 mg/L at 303, 313, 323, and 333 K for 1440 min. Using a UV−vis spectrophotometer (UV-2550, SHIMADZU), the absorbance of the solution was measured at a maximum wavelength of 464 nm to estimate the concentration of EB. The calibration curve was used to calculate the amount of EB present in an aqueous solution. Using following formula, the porous AEM's adsorption capacity was determined:

$$q_t = \frac{C_o - C_t}{W} \times V \tag{4}$$

where C_t and C_o denote the EB concentration at time t and the start of the experiment, respectively; the mass of the piece of porous AEM is represented by W; and the volume of the EB solution is represented by V.

2.5. Adsorption Isotherms. *2.5.1. Langmuir Isotherm.* The Langmuir isotherm assumes that the saturated monolayer of liquid molecules on the solid surface exhibits the greatest adsorption. It is presented as follows:[57,62]

$$\frac{C_e}{q_e} = \frac{1}{K_L Q_m} + \frac{C_e}{Q_m} \tag{5}$$

Here K_L is the Langmuir constant (L/mg), q_e is the quantity of dye adsorbed at equilibrium state of the system (mg/g), and C_e is the supernatant concentration at equilibrium state of the system (mg/L). The primary characteristic of the Langmuir adsorption isotherm is represented as the dimensionless constant separation factor R_L, which is given as follows:[62]

$$R_L = \frac{1}{1 + K_L C_o} \tag{6}$$

The isotherm's form is determined by the value of R_L, which might be linear ($R_L = 1$), unfavorable ($R_L > 1$), irreversible ($R_L = 0$), or otherwise favorable ($0 < R_L > 0$).[62]

2.5.2. Freundlich Isotherm. To analyze the heterogeneous system, the Freundlich isotherm is used as an empirical relation. It is expressed as follows:[63]

$$\log q_e = \log K_f + \frac{1}{n} \log C_e \tag{7}$$

The Freundlich isotherm constants used are n_f as well as K_f.

2.5.3. Temkin Isotherm. The Temkin isotherm is denoted as follows in its linear form:[57]

$$q_e = B_T \ln A_T + B_T \ln C_e \tag{8}$$

The adsorption heat and maximum binding energy are linked to the constants b_T and A_T, where $B_T = RT/b_T$, R is the gas constant (8.31 J/mol·K), and T is the absolute temperature (K), respectively.

2.6. Adsorption Kinetics. *2.6.1. Pseudo-First-Order Model.* The linear representation of the Lagergren pseudo-first-order rate is given as follows:[23,64]

$$\log(q_e - q_t) = \log q_e - \frac{k_1 t}{2.303} \tag{9}$$

The EB concentration adsorbed at equilibrium is q_e, q_t indicates EB concentration adsorbed at t, and k_1 (/min) is the pseudo-first-order model's constant.

2.6.2. Pseudo-Second-Order Model. In linear form, the pseudo-second-order kinetic model is shown as[57,64]

$$\frac{t}{q_t} = \frac{1}{k_2 q_e^2} + \frac{t}{q_e} \tag{10}$$

where k_2 (g/mg·min) is the rate constant for the pseudo-second-order model.

2.6.3. Elovich Model. The Elovich model is represented as[62,63]

$$q_t = \frac{1}{\beta} \ln(\alpha \beta) + \frac{1}{\beta} \ln t \tag{11}$$

Here the constants β (g/mg) and α (mg/g.min) are used. β is degree of surface coverage as well as the activation energy of chemisorption, and α is the rate of first adsorption.

2.6.4. Liquid Film Diffusion Model. The liquid film diffusion model is denoted as follows:[65]

$$\ln(1 - F) = -K_{fd} t \tag{12}$$

Here K_{fd} is the liquid film diffusion rate constant and $F = q_t/q_e$.

2.6.5. Modified Freundlich Equation. Kuo and Lotse presented the modified Freundlich equation at first as[23,57]

$$q_t = k C_o t^{1/m} \tag{13}$$

where, in order, k, C_o, t, and m stand for the Kuo−Lotse constant, the initial EB concentration in milligrams per liter (mg/L), the contact duration in minutes, and the adsorption rate constant (L/g·min). The provided linear form is

$$\ln q_t = \ln(k C_o) + \frac{1}{m} \ln t \tag{14}$$

2.6.6. Bangham Equation. The Bangham is denoted by means of[62,65]

$$\log \log \left(\frac{C_o}{C_o - q_t m} \right) = \log \left(\frac{k_o m}{2.303 V} \right) + \alpha \log t \tag{15}$$

In the above equation, V is the volume of the EB solution (mL), k_o is in mL/(g/L), $\alpha < 1$, and m is the mass of the porous AEM (g/L).

2.7. Adsorption Thermodynamics. We investigated the thermodynamics of EB adsorption onto the porous AEM by estimating enthalpy ($\Delta H°$), Gibb's free energy ($\Delta G°$), and entropy ($\Delta S°$) changes using the following equations:

$$\ln K_c = \frac{\Delta S^o}{R} - \frac{\Delta H^o}{RT} \tag{16}$$

$$K_c = \frac{C_a}{C_e} \tag{17}$$

$$\Delta G^o = \Delta H^o - T \Delta S^o \tag{18}$$

In the above equation, K_c is equilibrium constant, C_a is concentration adsorbed, C_e is equilibrium concentration, $\Delta G°$ stands for Gibbs free energy (kJ/mol) change, $\Delta H°$ is enthalpy (kJ/mol) change, and $\Delta S°$ is the entropy (J/mol·K) change.

3. RESULTS AND DISCUSSION

3.1. FTIR. We examined the production of the porous AEM with the use of FTIR spectroscopy. Figure 1 displays the obtained FTIR spectra of pure BPPO and porous AEM. The C−Br stretching vibration was the cause of the band that was identified at 750 cm^{-1} in the pure BPPO membrane.[56,66,67] The stretching vibration of C−N was indicated by a peak seen
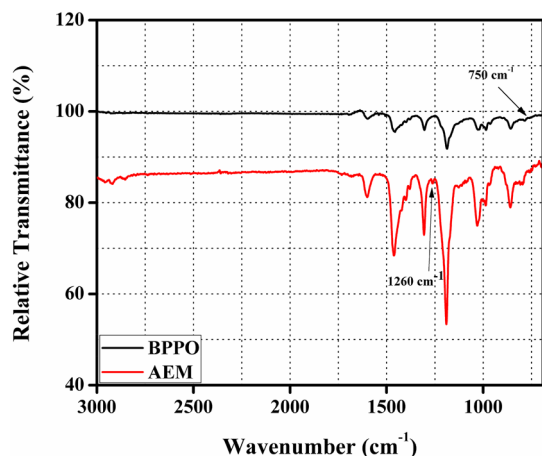
Figure 1. FTIR spectra of the fabricated porous AEM and pristine BPPO.

at 1260 cm^{-1} in the prepared porous AEM. Additionally, it is invisible in the clean BPPO membrane. In the porous AEM's ATR-FTIR spectrum, it had vanished. The TMA ion exchange moiety was added to the BPPO matrix to demonstrate the effectiveness of the AEM preparation.

3.2. Morphology. FE-SEM (Sirion 200, Hillsboro, OR, USA-based FEI Company) was used to study the morphology of the developed AEMs. Figure S2 displays SEM micrographs of the surface and cross-section of the created AEM. This study showed that the AEM had a porous structure. In addition, the

AEM was free from phase separation, cracks, or holes, demonstrating the excellent compatibility of the ion exchange moiety and polymer matrix. The cross-sectional micrograph contained a finger-like structure of pores as represented in Figure S2.

3.3. Thermal Stability. The produced AEM's thermal stability was demonstrated by thermogravimetric analysis (TGA). Temperatures between 30 and 700 °C were used to show thermal stability in a nitrogen environment. The generated AEM's TGA thermograph is shown in Figure S3. Three stages of weight loss were observed. Around 80−140 °C, the surface-adsorbed water on the AEMs began to evaporate, causing the first phase in the weight loss process.[68,69] The second phase of a weight loss occurred between 180 and 230 °C, at which point the quaternary ammonium group degraded into the polymer matrix.[46,70] Degradation of the polymer backbone, which corresponds to final weight loss step, was noted around 400 °C.[45,71] This demonstrated the prepared AEM's good thermal stability.

3.4. Ion Exchange Capacity, Water Absorption and Linear Swelling Ratio. Water absorption has a considerable effect on the properties of ion exchange membranes. Due to their necessity for ion transport and the fact that they are present inside the membrane matrix, water molecules also assisted in the separation of charged functional groups.[47,72] At room temperature, the produced AEM's determined water uptake was 240%. It implied that the generated porous AEM was effective at removing colors from sewage. The ion exchange capacity was calculated using the standard Mohr's
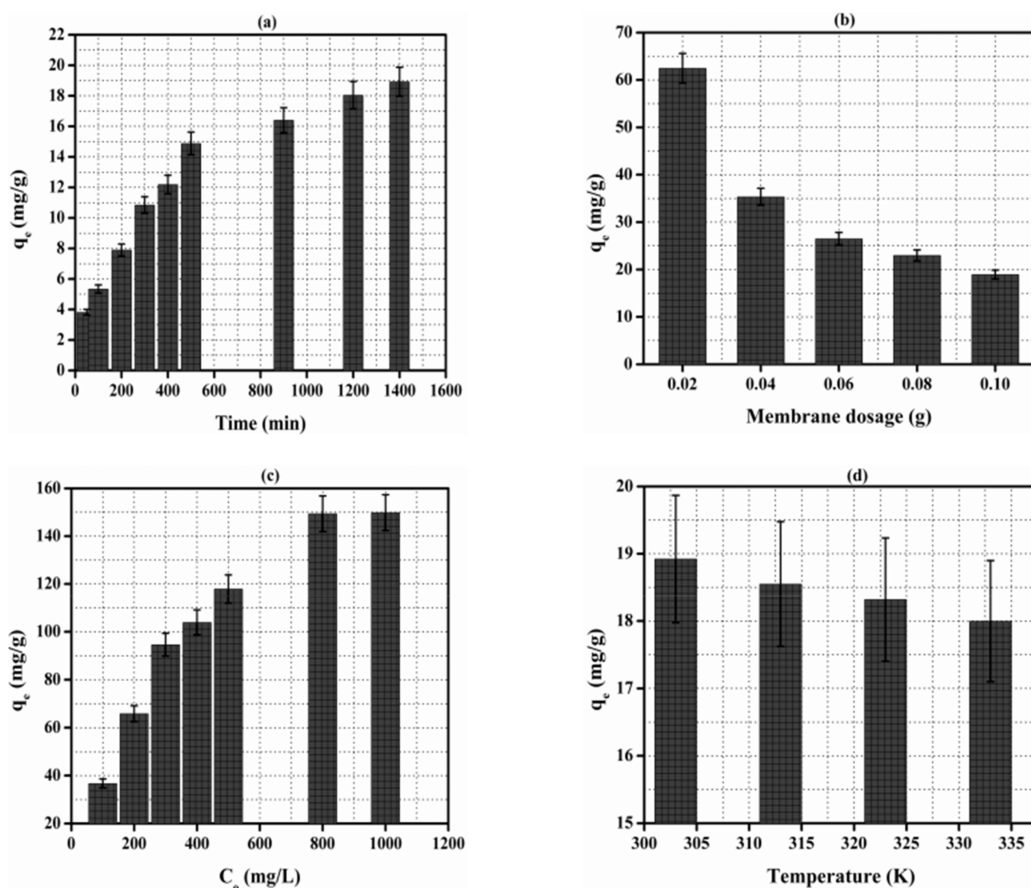
Figure 2. (a) Influence of contact duration, (b) membrane dosage, (c) EB starting concentration, and (d) temperature on EB adsorption capacity.

method. The ion exchange membrane's importance in relation to hydrophilicity and transport characteristics is a key factor.[67] The measured IEC value of the prepared AEM was 1.45 mg/g. At room temperature, the AEM's linear swelling ratio was studied. Measured LER value was 9.0%. It showed that the developed AEM exhibited a higher swelling resistance suitable for their electrochemical properties.

3.5. Impact of Operational Variables on Wastewater EB Removal.
In this Article, the operational elements that have an impact on the amount of EB that the developed porous AEM discharges from wastewater are thoroughly illustrated. The effect of contact duration on EB% discharge from wastewater is indicated in Figure 2a. The EB discharge was shown to increase with contact time at room temperature. In addition, the EB removal was fast at the beginning stage due to the presence of excessive active sites on the porous AEM and declined with the passage of time. From these results, an equilibrium was found after 1400 min. This optimized time was utilized to conduct further experiments.

Adsorbent amounts have significant effects on the discharge of dyes from wastewater. These effects were investigated by increasing the porous AEM mass at room temperature from 0.01 to 0.05 g, and the results are presented in Figure. 2b. As the porous AEM mass increased at room temperature from 0.01 to 0.05 g, the adsorption capacity of EB onto the porous membrane was shown to decline. It was due to limited EB concentration an the aqueous solution.[19]

The influence of the EB starting concentration on its percentage release from wastewater was also investigated at room temperature. Figure 2c demonstrates the effect of the EB starting concentration on the waste product elimination percentage. The findings revealed that increasing the concentration of first colorant in solution increased EB's adsorption capacity on the synthetic porous AEM. The problem was caused by the greater concentration of EB in the mixture, which enhanced the molecules' ability to move from the solution to the porous AEM side. The porous AEM surface and EB molecules interacted more often. It suggested that the porous AEM's capacity for adsorption was positively influenced by the EB starting concentration.[19,59]

By adjusting the temperature from 273 to 333 K, the impact of temperature on the EB adsorption capacity was investigated. Figure 2d illustrates the impact of temperature on the EB adsorption capacity. The EB adsorption capacity was shown to decrease with the temperature increase. From here, we conclude that the discharge of EB from wastewater by the developed porous AEM was an exothermic process.

3.6. Adsorption Isotherms.
To explain EB adsorption onto the produced porous AEM, several isotherm models, including Temkin, Langmuir, and Freundlich models, were utilized. The measured parameters are represented in Table 1, and their plots are displayed in Figure. 3. The isotherm of the Langmuir curve used for the adsorption of EB on the porous AEM is presented in Figure 3a. Table 1 provides the derived values for the Langmuir isotherm. The correlation coefficient value ($R^2 = 0.992$) that is close to unity shows that the Langmuir isotherm was obeyed by EB adsorption onto the generated porous AEM. The calculated R_L (0.05−0.34) value indicated that the procedure of EB adsorption was successful. In Figure 3b, the Freundlich isotherm for EB adsorption is shown. Table 1 lists the calculated values of its components. The findings showed that EB adhered to the produced porous AEM according to the Freundlich adsorption isotherm. Values

Table 1. EB Adsorption onto the Created Porous AEM Performed Using the Determined Isotherms of Adsorption Parameters

isotherms of adsorption	determined factors			
Langmuir isotherm	q_e = 162.10	K_L = 1.90×10^{-2}	R^2 = 0.992	R_L = 0.050−0.34
Freundlich isotherm	n = 3.10	k_F = 20.49	R^2 = 0.957	
Temkin isotherm	A_T = 0.40	b_T = 90.15	R^2 = 0.974	

between 1 and 2 indicated weak adsorption, and those less than 1 indicated strong adsorption for the Freundlich constant n, which had a range of 2−10.[57,59] In addition, Figure 3c shows the Temkin isotherm plot for EB adsorption. Its measured b_T and A_T values are shown in Table 1. The Temkin isotherm's correlation coefficient ($R^2 = 0.974$) was lower than that of the Langmuir isotherm; therefore, it was recognized that it was not practical to discuss EB adsorption onto the created porous AEM using this Temkin isotherm.

3.7. Adsorption Kinetics.
With the help of kinetic models, the expected mechanism and the adsorption pathway being followed can be predicted.[73] Adsorption process is expected to follow a variety of mechanisms, based on which it can be deduced if the adsorption process is physical or chemical in nature. Generally, the pseudo-first-order model describes diffusion-based adsorption, while the second-order model is more specifically followed in case of chemical adsorption, which involves the exchange of electrons between the membrane and adsorbate.[73,74] For EB adsorption onto the developed porous AEM from wastewater, adsorption kinetics were illustrated by applying several kinetics models. The graphs of the kinetic models used are shown in Figure 4, and Table 2 contains calculated kinetic factors. According to the obtained data, the pseudo-second-order model presented best fit, which suggests that the efficiency of the membrane to adsorb the solute mainly depends on its uptake capacity instead of the solute's concentration.[75] For the prepared porous AEM, the application of the pseudo-second-order model represents the interaction between dye molecules and the ion exchange group of the prepared porous AEM.[76] Therefore, the adsorption system was chemical adsorption. It was noted that the EB adsorption process onto the porous was best fitted to the pseudo-second-order model with a chemical adsorption mechanism.[76−78] The pseudo-second-order kinetic model has been strongly utilized to dictate chemisorption in various sorption systems. Besides, the Elovich model was not able to describe EB adsorption onto the porous AEM (Table 2, Figure 4).

Similarly, the liquid film diffusion model ($R^2 = 0.980$) and modified Freundlich equation ($R^2 = 0.969$) were not as favorable as the pseudo-second-order model, making them an unsuitable choice for study (Figure 5, Table 2). Figure 5c shows the EB adsorption curve of the Bangham equation. The plot's lack of linear curves indicates that there are other rate-regulating processes than the adsorbate's (EB) diffusion into the adsorbent's pores (the generated porous AEM).[23,65] Both film and pore diffusion were crucial to different extents for EB adsorption from wastewater onto the porous AEM.[58,79]

3.8. Adsorption Thermodynamics.
To conduct an adsorption thermodynamics analysis for EB adsorption onto the produced porous AEM, the values for entropy ($\Delta S°$),
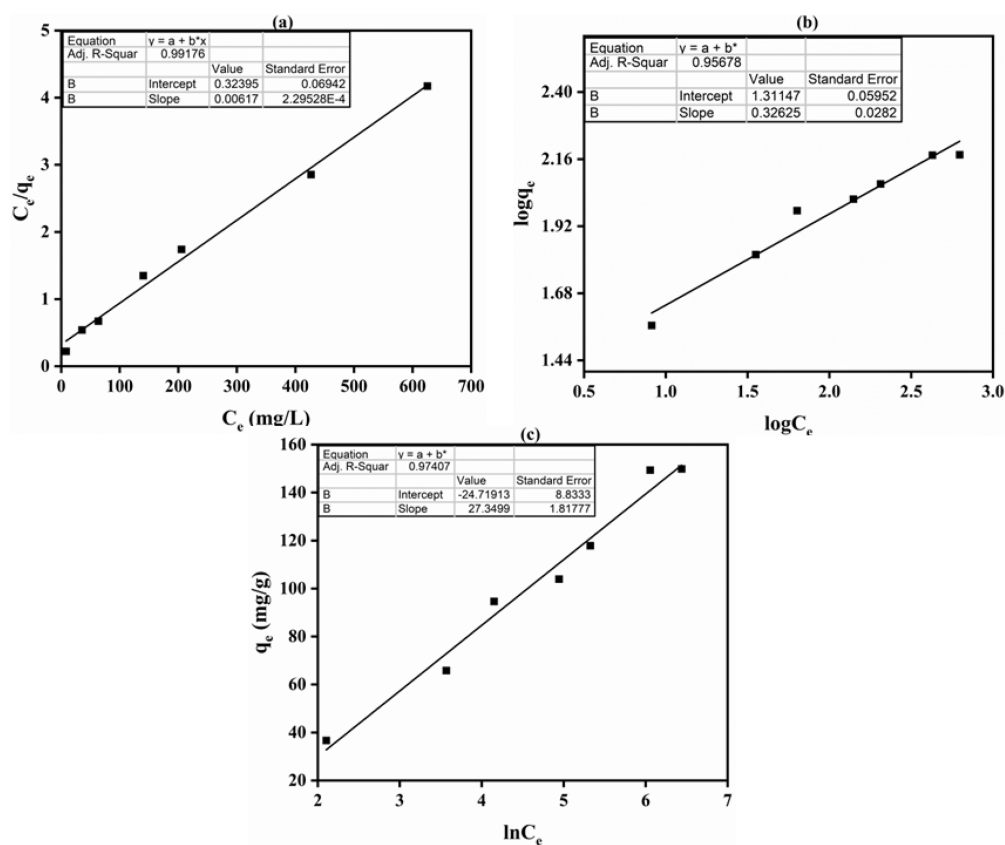
Figure 3. (a) Langmuir isotherm, (b) Freundlich isotherm, and (c) Temkin isotherm for EB adsorption onto the developed porous AEM from wastewater.
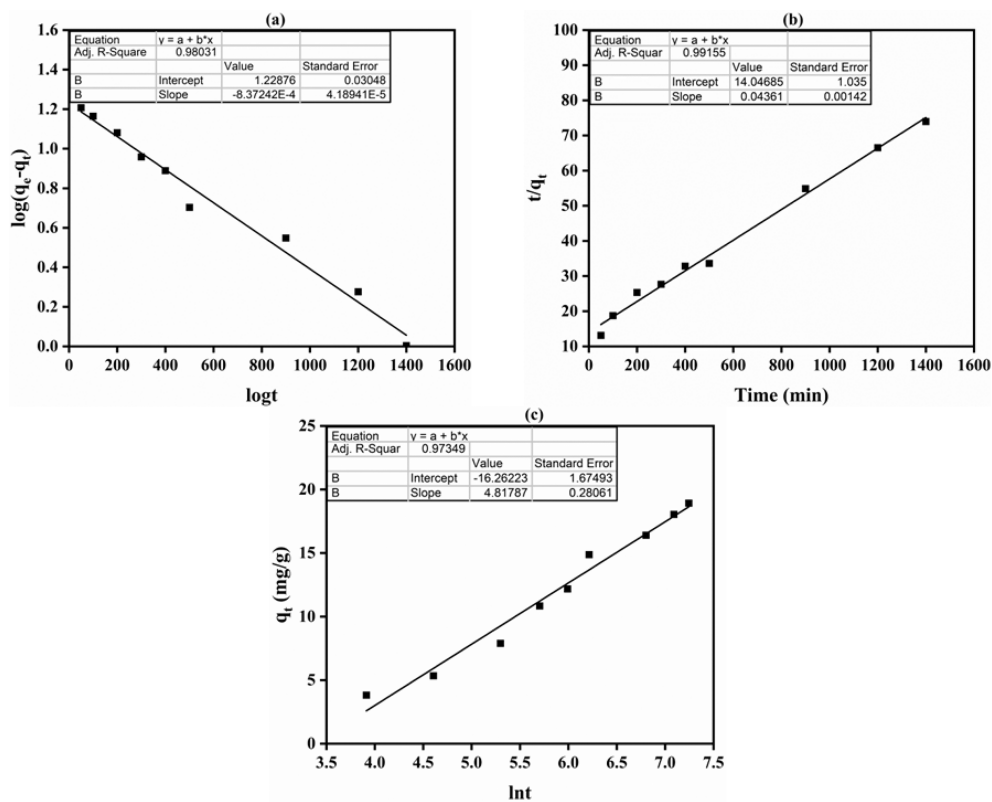
Figure 4. (a) Plot of pseudo-first-order, (b) pseudo-second-order, and (c) Elovich models for EB adsorption onto the developed porous AEM from wastewater.

Table 2. Determined Adsorption Kinetic Parameters for EB on the Created Porous AEM

models for kinetic adsorption	parameter measurements		
model of pseudo-first order	q_e = 16.93	k_1 = 8.37×10^{-4}	R^2 = 0.980
model of pseudo-second-order	q_e = 22.93	k_2 = 1.35×10^{-4}	R^2 = 0.992
Elovich model	α = 0.16	β = 0.21	R^2 = 0.973
liquid film diffusion model	K_{fd} = 1.93×10^{-3}	C_{fd} = −0.162	R^2 = 0.980
modified Freundlich equation	m = 2.02	k = 0.012	R^2 = 0.969
Bangham equation	α = 0.50	k_o = 0.462	R^2 = 0.969

Figure 6. Graph sjpwomg the relationship between $1/T$ and ln Kc for EB adsorption onto the created porous AEM from wastewater.

Table 3. Determined Thermodynamic Parameter Values for EB Adsorption onto the Porous AEM

T (K)	$\Delta G°$ (kJ/mol)	$\Delta H°$ (kJ/mol)	$\Delta S°$ (kJ/mol)
303	−7.04		
313	−6.73	−16.60	−0.032
323	−6.41		
333	−6.10		

enthalpy ($\Delta H°$), and Gibb's free energy ($\Delta G°$) were determined. The graph between ln K_c and $1/T$ for EB adsorption is indicated in Figure 6. Table 3 lists the thermodynamic factors values. Generally, a positive $\Delta G°$ shows that an external source of energy is needed during the adsorption process.[80] Simultaneously, a negative $\Delta G°$ value shows the feasibility of the adsorption process and its spontaneous nature without the requirement for an external energy source.[80] The negative value of $\Delta G°$ (Gibb's free energy) at all temperatures was obtained for EB adsorption onto the porous AEM, demonstrating that EB adsorption occurred spontaneously onto the porous AEM without the requirement of external energy.[78] As seen from Table 3, the EB adsorption onto the porous AEM was an exothermic process because of the negative enthalpy value ($\Delta H°$ = −16.60 kJ/mol).[23,63] Additionally, the EB adsorption onto the resulting porous AEM from wastewater was observed to result in a

reduction in arbitrariness at the adsorbate−adsorbent interface, leading to a negative entropy value.[63,81]
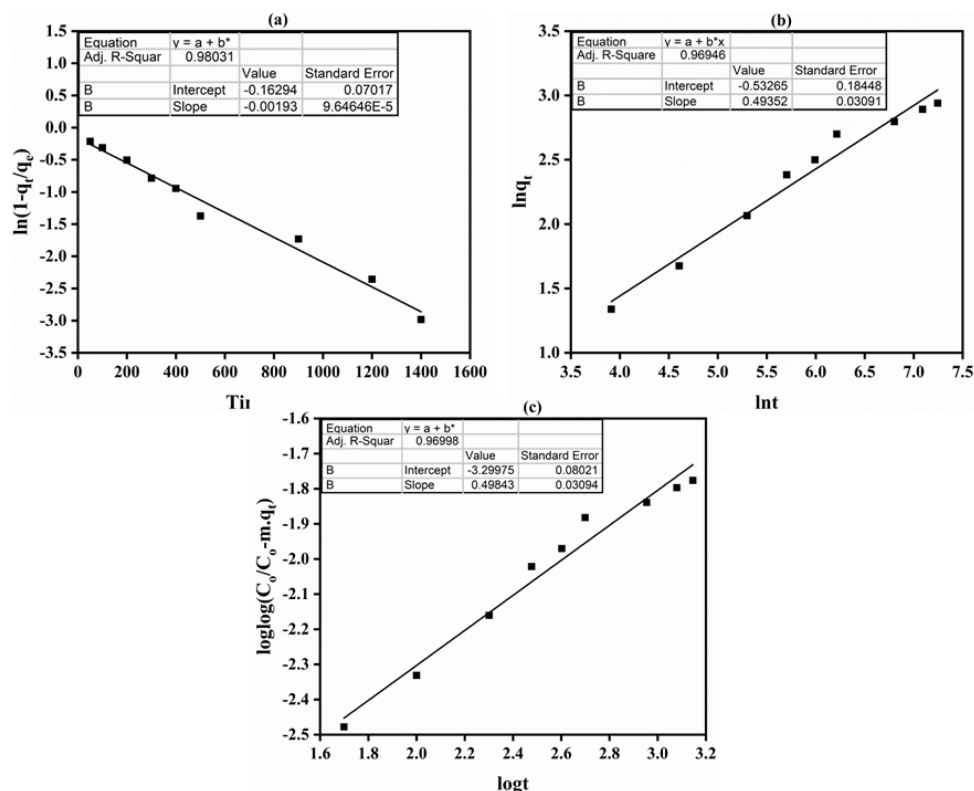
Figure 5. (a) Liquid film diffusion model, (b) modified Freundlich equation, and (c) Bangham equation for EB adsorption onto the developed porous AEM from wastewater.

4. CONCLUSION

This Article provided a detailed description of the phase inversion approach utilized to construct the porous AEM. The effective production of the porous AEM from the interaction of BPPO and TMA was verified by FTIR spectroscopy. It showed excellent thermal stability as well as a porous structure. It exhibited an IEC of 1.45 mg/g, a LER of 9.0%, and a W_R of 240% at 25 °C. It was discovered that EB adsorption onto the porous AEM increased with time and the initial EB concentration, while it decreased with the AEM dose and temperature. According to the isotherm analysis, EB adsorption onto the porous AEM fit the Langmuir isotherm. The pseudo-second-order kinetics of EB adsorption is suitable according to the adsorption kinetics. Thermodynamic analysis revealed that EB adsorption onto the porous AEM was an exothermic and spontaneous process. It was shown how effectively the porous AEM generated could be used as an adsorbent to extract EB from wastewater.

ASSOCIATED CONTENT

Supporting Information

The Supporting Information is available free of charge at https://pubs.acs.org/doi/10.1021/acsomega.3c06827.

Reaction scheme of fabricated porous AEM synthesis, cross-section and surface micrographs of the fabricated porous AEM, and TGA thermograph of pure BPPO and the fabricated porous AEM (PDF)

AUTHOR INFORMATION

Corresponding Author

Noureddine Elboughdiri − *Chemical Engineering Department, College of Engineering, University of Ha'il, Ha'il 81441, Saudi Arabia; Chemical Engineering Process Department, National School of Engineers Gabes, University of Gabes, Gabes 6029, Tunisia;* orcid.org/0000-0003-2923-3062; Email: ghilaninouri@yahoo.fr

Authors

Muhammad Imran Khan − *Research Institute of Sciences and Engineering (RISE), University of Sharjah, Sharjah 27272, United Arab Emirates*

Abdallah Shanableh − *Research Institute of Sciences and Engineering (RISE), University of Sharjah, Sharjah 27272, United Arab Emirates*

Asma Manzoor − *Department of Chemistry, The Government Sadiq College Women University, Bahawalpur 63100, Pakistan*

Suryyia Manzoor − *Institute of Chemical Sciences, Bahauddin Zakariya University, Multan 60000, Pakistan*

Nosheen Farooq − *Department of Chemistry, The Government Sadiq College Women University, Bahawalpur 63100, Pakistan*

Jannat Suleman − *Department of Chemistry, The Women University Multan, Multan 60000, Pakistan*

Hadia Sarwar − *Department of Chemistry, The Government Sadiq College Women University, Bahawalpur 63100, Pakistan*

Mhamed Benaissa − *Chemical Engineering Department, College of Engineering, University of Ha'il, Ha'il 81441, Saudi Arabia;* orcid.org/0000-0002-5639-6169

Yacine Benguerba − *Laboratoire de Biopharmacie Et Pharmacotechnie (LBPT), Université Ferhat ABBAS Sétif-1, Sétif 19000, Algeria; Chemical Engineering Department, College of Engineering, University of Ha'il, Ha'il 81441, Saudi Arabia;* orcid.org/0000-0002-8251-9724

Complete contact information is available at:
https://pubs.acs.org/10.1021/acsomega.3c06827

Notes

The authors declare no competing financial interest.

ACKNOWLEDGMENTS

REFERENCES

(1) Gong, R.; Sun, Y.; Chen, J.; Liu, H.; Yang, C. Effect of chemical modification on dye adsorption capacity of peanut hull. *Dyes Pigm.* 2005, 67 (3), 175−181.

(2) Ong, S. T.; Lee, C. K.; Zainal, Z. Removal of basic and reactive dyes using ethylenediamine modified rice hull. *Bioresourc. Technol.* 2007, 98 (15), 2792−2799.

(3) Ho, Y.; Chiang, C. Sorption studies of acid dye by mixed sorbents. *Adsorption* 2001, 7 (2), 139−147.

(4) Hameed, B.; El-Khaiary, M. Equilibrium, kinetics and mechanism of malachite green adsorption on activated carbon prepared from bamboo by K_2CO_3 activation and subsequent gasification with CO_2. *J. Hazard. Mater.* 2008, 157 (2), 344−351.

(5) Gupta, V. K.; Ali, I; Suhas; Mohan, D. Equilibrium uptake and sorption dynamics for the removal of a basic dye (basic red) using low-cost adsorbents. *J. Colloid Interface Sci.* 2003, 265 (2), 257−264.

(6) Chen, H.; Zhao, J. Adsorption study for removal of Congo red anionic dye using organo-attapulgite. *Adsorption* 2009, 15 (4), 381−389.

(7) Park, K. H.; Parhi, P. K.; Kang, N.-H. Studies on Removal of Low Content Copper from the Sea Nodule Aqueous Solution using the Cationic Resin TP 207. *Sep. Sci. Technol.* 2012, 47 (10), 1531−1541.

(8) Mohapatra, R. K.; Parhi, P. K.; Pandey, S.; Bindhani, B. K.; Thatoi, H.; Panda, C. R. Active and passive biosorption of Pb(II)using live and dead biomass of marine bacterium Bacillus xiamenensis PbRPSD202: Kinetics and isotherm studies. *J. Environ. Manage.* 2019, 247, 121−134.

(9) Tabatabaee, M.; Mirrahimi, S. A. Photodegradation of Dye Pollutant on Ag/ZnO Nanocatalyst under UV-irradiation. *Orien. J. Chem.* 2011, 27 (1), 65.

(10) Caprarescu, S.; Miron, A. R.; Purcar, V.; Radu, A.-L.; Sarbu, A.; Ion-Ebrasu, D.; Atanase, L.-I.; Ghiurea, M. Efficient removal of Indigo Carmine dye by a separation process. *Water Sci. Technol.* 2016, 74 (10), 2462−2473.

(11) Khan, M. I.; Shanableh, A.; Nasir, N.; Shahida, S. Adsorptive removal of methyl orange from wastewaters by the commercial anion exchange membrane EPTAC. *Desal. Water Treat.* 2021, 234, 245−254.

(12) Modrogan, C.; Căprărescu, S.; Dăncilă, A. M.; Orbuleţ, O. D.; Grumezescu, A. M.; Purcar, V.; Radiţoiu, V.; Fierascu, R. C. Modified Composite Based on Magnetite and Polyvinyl Alcohol: Synthesis, Characterization, and Degradation Studies of the Methyl Orange Dye from Synthetic Wastewater. *Polymers* 2021, 13 (22), 3911.

(13) Obotey Ezugbe, E.; Rathilal, S. Membrane Technologies in Wastewater Treatment: A Review. *Membranes* 2020, 10 (5), 89.

(14) Caprarescu, S.; Miron, A. R.; Purcar, V.; Radu, A. L.; Sarbu, A.; Nicolae, C. A.; Pascu, M.; Ion-Ebrasu, D.; Raditoiu, V. Treatment of Crystal Violet from Synthetic Solution Using Membranes Doped with Natural Fruit Extract. *CLEAN - Soil Air Water* 2018, 46 (7), 1700413.

(15) Gan, L.; Cheng, Y.; Palanisami, T.; Chen, Z.; Megharaj, M.; Naidu, R. Pathways of reductive degradation of crystal violet in

wastewater using free-strain Burkholderia vietnamiensis C09V. *Environ. Sci. Poll. Res.* **2014**, *21* (17), 10339−10348.

(16) de Oliveira Guidolin, T.; Possolli, N. M.; Polla, M. B.; Wermuth, T. B.; Franco de Oliveira, T.; Eller, S.; Klegues Montedo, O. R.; Arcaro, S.; Cechinel, M. A. P. Photocatalytic pathway on the degradation of methylene blue from aqueous solutions using magnetite nanoparticles. *J. Clean. Prod.* **2021**, *318*, 128556.

(17) Lin, C.-H.; Gung, C.-H.; Wu, J.-Y.; Suen, S.-Y. Cationic dye adsorption using porous composite membrane prepared from plastic and plant wastes. *J. Taiwan Inst. Chem. Eng.* **2015**, *51*, 119−126.

(18) Joo, S.-H.; Kim, Y.-U.; Kang, J.-G.; Kumar, J. R.; Yoon, H.-S.; Parhi, P. K.; Shin, S. M. Recovery of Rhenium and Molybdenum from Molybdenite Roasting Dust Leaching Solution by Ion Exchange Resins. *Mater. Trans.* **2012**, *53* (11), 2034−2037.

(19) Khan, M. I.; Shanableh, A.; Fernandez, J.; Lashari, M. H.; Shahida, S.; Manzoor, S.; Zafar, S.; ur Rehman, A.; Elboughdiri, N. Synthesis of DMEA-Grafted Anion Exchange Membrane for Adsorptive Discharge of Methyl Orange from Wastewaters. *Membranes* **2021**, *11* (3), 166.

(20) Khan, M. I.; Akhtar, S.; Zafar, S.; Shaheen, A.; Khan, M. A.; Luque, R.; Rehman, A. Removal of Congo Red from Aqueous Solution by Anion Exchange Membrane (EBTAC): Adsorption Kinetics and Thermodynamics. *Materials* **2015**, *8* (7), 4147−4161.

(21) Yagub, M. T.; Sen, T. K.; Afroze, S.; Ang, H. M. Dye and its removal from aqueous solution by adsorption: A review. *Adv. Coll. Interface Sci.* **2014**, *209*, 172−184.

(22) Janoš, P.; Buchtová, H.; Rýznarová, M. Sorption of dyes from aqueous solutions onto fly ash. *Water Res.* **2003**, *37* (20), 4938−4944.

(23) Khan, M. I.; Lashari, M. H.; Khraisheh, M.; Shahida, S.; Zafar, S.; Prapamonthon, P.; ur Rehman, A.; Anjum, S.; Akhtar, N.; Hanif, F. Adsorption kinetic, equilibrium and thermodynamic studies of Eosin-B onto anion exchange membrane. *Desal. Water Treat.* **2019**, *155*, 84−93.

(24) Başar, C. A. Applicability of the various adsorption models of three dyes adsorption onto activated carbon prepared waste apricot. *J. Hazard. Mater.* **2006**, *135* (1), 232−241.

(25) Crini, G. Non-conventional low-cost adsorbents for dye removal: a review. *Bioresourc. Technol.* **2006**, *97* (9), 1061−1085.

(26) Sumanjit; Walia, T. P. S. Use of dairy sludge for the removal of some basic dyes. *J. Environ. Eng. Sci.*. **2008**, *7* (5), 433−438.

(27) Sun, Q.; Yang, L. The adsorption of basic dyes from aqueous solution on modified peat−resin particle. *Water Res.* **2003**, *37* (7), 1535−1544.

(28) Kumar, K. V.; Porkodi, K. Batch adsorber design for different solution volume/adsorbent mass ratios using the experimental equilibrium data with fixed solution volume/adsorbent mass ratio of malachite green onto orange peel. *Dyes Pigm.* **2007**, *74* (3), 590−594.

(29) Vijayalakshmi, P.; Bala, V. S. S.; Thiruvengadaravi, K. V.; Panneerselvam, P.; Palanichamy, M.; Sivanesan, S. Removal of Acid Violet 17 from Aqueous Solutions by Adsorption onto Activated Carbon Prepared from Pistachio Nut Shell. *Sep. Sci. Technol.* **2010**, *46* (1), 155−163.

(30) Sumanjit; Prasad, N. Adsorption of dyes on rice husk ash. *Indian J. Chem.* **2001**, *40* (4), 388−391.

(31) Kaur, S.; Mahajan, R. K.; Rani, S.; Walia, T. P. S.; Kaur, R. Adsorptive removal of five acid dyes using various unconventional adsorbents. *J. Surf. Sci. Technol.* **2010**, *26* (1), 77−93.

(32) Ma, J.-W.; Wang, H.; Wang, F.-Y.; Huang, Z.-H. Adsorption of 2,4-dichlorophenol from Aqueous Solution by a New Low-Cost Adsorbent−Activated Bamboo Charcoal. *Sep. Sci. Technol.* **2010**, *45* (16), 2329−2336.

(33) Jain, S.; Jayaram, R. V. Adsorption of Phenol and Substituted Chlorophenols from Aqueous Solution by Activated Carbon Prepared from Jackfruit (artocarpus heterophyllus) Peel-Kinetics and Equilibrium Studies. *Sep. Sci. Technol.* **2007**, *42* (9), 2019−2032.

(34) Belala, Z.; Jeguirim, M.; Belhachemi, M.; Addoun, F.; Trouve, G. Biosorption of copper from aqueous solutions by date stones and palm-trees waste. *Environ. Chem. Letters* **2011**, *9* (1), 65−69.

(35) Lin, Y.-F.; Chen, H.-W.; Chien, P.-S.; Chiou, C.-S.; Liu, C.-C. Application of bifunctional magnetic adsorbent to adsorb metal cations and anionic dyes in aqueous solution. *J. Hazard. Mater.* **2011**, *185* (2), 1124−1130.

(36) Dural, M. U.; Cavas, L.; Papageorgiou, S. K.; Katsaros, F. K. Methylene blue adsorption on activated carbon prepared from Posidonia oceanica (L.) dead leaves: Kinetics and equilibrium studies. *Chem. Eng. J.* **2011**, *168* (1), 77−85.

(37) Xiao, S.; Shen, M.; Guo, R.; Huang, Q.; Wang, S.; Shi, X. Fabrication of multiwalled carbon nanotube-reinforced electrospun polymer nanofibers containing zero-valent iron nanoparticles for environmental applications. *J. Mater. Chem.* **2010**, *20* (27), 5700−5708.

(38) Wesenberg, D.; Kyriakides, I.; Agathos, S. N. White-rot fungi and their enzymes for the treatment of industrial dye effluents. *Biotechnol. Adv.* **2003**, *22* (1), 161−187.

(39) Wu, J.-S.; Liu, C.-H.; Chu, K. H.; Suen, S.-Y. Removal of cationic dye methyl violet 2B from water by cation exchange membranes. *J. Membr. Sci.* **2008**, *309* (1−2), 239−245.

(40) Chiu, H.-C.; Liu, C.-H.; Chen, S.-C.; Suen, S.-Y. Adsorptive removal of anionic dye by inorganic−organic hybrid anion-exchange membranes. *J. Membr. Sci.* **2009**, *337* (1), 282−290.

(41) Khan, M. I.; Ansari, T. M.; Zafar, S.; Buzdar, A. R.; Khan, M. A.; Mumtaz, F.; Prapamonthon, P.; Akhtar, M. Acid green-25 removal from wastewater by anion exchange membrane: Adsorption kinetic and thermodynamic studies. *Membr. Water Treat.* **2018**, *9* (2), 79−85.

(42) Khan, M. I.; Khan, M. A.; Zafar, S.; Ashiq, M. N.; Athar, M.; Qureshi, A. M.; Arshad, M. Kinetic, equilibrium and thermodynamic studies for the adsorption of methyl orange using new anion exchange membrane (BII). *Desal. Water Treat.* **2017**, *58*, 285−297.

(43) Khan, M. I.; Zafar, S.; Khan, M. A.; Buzdar, A. R.; Prapamonthon, P. Adsorption kinetic, equilibrium and thermodynamic study for the removal of Congo Red from aqueous solution. *Desal. Water Treat.* **2017**, *98*, 294−305.

(44) Khan, M. I.; Wu, L.; Mondal, A. N.; Yao, Z.; Ge, L.; Xu, T. Adsorption of methyl orange from aqueous solution on anion exchange membranes: Adsorption kinetics and equilibrium. *Membr. Water Treat.* **2016**, *7* (1), 23−38.

(45) Khan, M. I.; Wu, L.; Hossain, M. M.; Pan, J.; Ran, J.; Mondal, A. N.; Xu, T. Preparation of diffusion dialysis membrane for acid recovery via a phase-inversion method. *Membr. Water Treat.* **2015**, *6* (5), 365−378.

(46) Khan, M. I.; Mondal, A. N.; Cheng, C.; Pan, J.; Emmanuel, K.; Wu, L.; Xu, T. Porous BPPO-based membranes modified by aromatic amine for acid recovery. *Sep. Purif. Technol.* **2016**, *157*, 27−34.

(47) Khan, M. I.; Shanableh, A.; Khraisheh, M.; AlMomani, F. Synthesis of Porous BPPO-Based Anion Exchange Membranes for Acid Recovery via Diffusion Dialysis. *Membranes* **2022**, *12* (1), 95.

(48) Khan, M. I.; Fernandez-Garcia, J.; Zhu, Q.-L. Fabrication of doubly charged anion-exchange membranes for enhancing hydroxide conductivity. *Sep. Sci. Technol.* **2021**, *56*, 1589−1600.

(49) Khan, M. I.; Mondal, A. N.; Emmanuel, K.; Hossain, M. M.; Afsar, N. U.; Wu, L.; Xu, T. Preparation of pyrrolidinium-based anion-exchange membranes for acid recovery via diffusion dialysis. *Sep. Sci. Technol.* **2016**, *51* (11), 1881−1890.

(50) Khan, M. I.; Su, J.; Lichtfouse, E.; Guo, L. Higher efficiency of triethanolamine-grafted anion exchange membranes for acidic waste-water treatment. *Desal. Water Treat.* **2020**, *197*, 41−51.

(51) Khan, M. I.; Li, X.; Fernandez-Garcia, J.; Lashari, M. H.; ur Rehman, A.; Elboughdiri, N.; Kolsi, L.; Ghernaout, D. Effect of Different Quaternary Ammonium Groups on the Hydroxide Conductivity and Stability of Anion Exchange Membranes. *ACS Omega* **2021**, *6* (12), 7994−8001.

(52) Khan, M. I.; Khraisheh, M.; AlMomani, F. Innovative BPPO Anion Exchange Membranes Formulation Using Diffusion Dialysis-Enhanced Acid Regeneration System. *Membranes* **2021**, *11* (5), 311.

(53) Khan, M. I.; Su, J.; Guo, L. Preparation and characterization of high-performance anion exchange membranes for acid recovery. *Desal. Water Treat.* **2021**, *209*, 144−154.

(54) Khan, M. I.; Su, J. J.; Guo, J. Development of high performance anion exchange membranes for diffusion dialysis process. *Desal. Water Treat.* **2021**, *221*, 281−290.

(55) Khan, M. I.; Su, J.; Guo, L. Development of triethanolamine functionalized-anion exchange membrane for adsorptive removal of methyl orange from aqueous solution. *Desalination and Water Treatment* **2021**, *209*, 342−352.

(56) Khan, M. I.; Khraisheh, M.; Almomani, F. Fabrication and characterization of pyridinium functionalized anion exchange membranes for acid recovery. *Sci. Total Environ.* **2019**, *686*, 90−96.

(57) Arif, S.; Zafar, S.; Khan, M. I.; Manzoor, S.; Shanableh, A.; Garcia, J. F.; Hayat, M. Removal of chromium (VI) by commercial anion exchange membrane BII from an aqueous solution: Adsorption kinetic, equilibrium and thermodynamic studies. *Inor. Chem. Commun.* **2023**, *152*, 110696.

(58) Khan, M. I.; Shanableh, A.; Alfantazi, A. M.; Lashari, M. H.; Manzoor, S.; Anwer, R.; Farooq, N.; Harraz, F. A.; Alsaiari, M.; Faisal, M. Application of QPPO/PVA based commercial anion exchange membrane as an outstanding adsorbent for the removal of Eosin-B dye from wastewaters. *Chemosphere* **2023**, *321*, 138006.

(59) Khan, M. I.; Shanableh, A.; Elboughdiri, N.; Lashari, M. H.; Manzoor, S.; Shahida, S.; Farooq, N.; Bouazzi, Y.; Rejeb, S.; Elleuch, Z.; Kriaa, K.; ur Rehman, A. Adsorption of Methyl Orange from an Aqueous Solution onto a BPPO-Based Anion Exchange Membrane. *ACS Omega* **2022**, *7* (30), 26788−26799.

(60) Khan, M. I.; Elboughdiri, N.; Shanableh, A.; Lashari, M. H.; Shahida, S. Application of the commercial anion exchange membrane for adsorptive removal of Eriochrome Black-T from aqueous solution. *Desal. Water Treat.* **2022**, *252*, 437−448.

(61) Iqbal, M.; Zafar, S.; Khan, M. I.; Shahida, S.; ur Rehman, H.; Iqbal, M.; Shanableh, A.; Javed, T. Utilization of Mangifera indica leaves powder as a cost-effective adsorbent for the removal of eosin yellow from wastewater. *Desal. Water Treat.* **2023**, *306*, 236−244.

(62) Ayyaril, S. S.; Khan, M. I.; Shanableh, A.; Bhattacharjee, S.; de Oliveira, D. M. Fabrication of nano-activated charcoal incorporated sodium alginate-based cross-linked membrane for Rhodamine B adsorption from an aqueous solution. *Desal. Water Treat.* **2022**, *278*, 239−250.

(63) Almanassra, I. W.; Khan, M. I.; Atieh, M. A.; Shanableh, A. Adsorption of lead ions from an aqueous solution onto NaOH-modified rice husk. *Desal. Water Treat.* **2022**, *262*, 152−167.

(64) Zafar, S.; Khan, M. I.; Khraisheh, M.; Shahida, S.; Javed, T.; Mirza, M. L.; Khalid, N. Use of rice husk as an efective sorbent for the removal of cerium ions from aqueous solution: kinetic, equilibrium and thermodynamic studies. *Desal. Water Treat.* **2019**, *150*, 124−135.

(65) Zafar, S.; Khan, M. I.; Khraisheh, M.; Lashari, M. H.; Shahida, S.; Azhar, M. F.; Prapamonthon, P.; Mirza, M. L.; Khalid, N. Kinetic, equilibrium and thermodynamic studies for adsorption of nickel ions onto husk of Oryza sativa. *Desal. Water Treat.* **2019**, *167*, 277−90.

(66) Khan, M. I.; Shanableh, A.; Manzoor, S.; Fernandez, J.; Osman, S. M.; Luque, R. Design of tropinium-functionalized anion exchange membranes for acid recovery via diffusion dialysis process. *Environ. Res.* **2023**, *229*, 115932.

(67) Khan, M. I.; Shanableh, A.; Osman, S. M.; Lashari, M. H.; Manzoor, S.; Rehman, A. u.; Luque, R. Fabrication of trimethylphosphine-functionalized anion exchange membranes for desalination application via electrodialysis process. *Chemosphere* **2022**, *308*, 136330.

(68) Khan, M. I.; Zheng, C.; Mondal, A. N.; Hossain, M. M.; Wu, B.; Emmanuel, K.; Wu, L.; Xu, T. Preparation of anion exchange membranes from BPPO and dimethylethanolamine for electrodialysis. *Desalination* **2017**, *402*, 10−18.

(69) Khan, M. I.; Luque, R.; Prinsen, P.; ur Rehman, A.; Anjum, S.; Nawaz, M.; Shaheen, A.; Zafar, S.; Mustaqeem, M. BPPO-Based Anion Exchange Membranes for Acid Recovery via Diffusion Dialysis. *Materials* **2017**, *10* (3), 266.

(70) Khan, M. I.; Mondal, A. N.; Tong, B.; Jiang, C.; Emmanuel, K.; Yang, Z.; Wu, L.; Xu, T. Development of BPPO-based anion exchange membranes for electrodialysis desalination applications. *Desalination* **2016**, *391*, 61−68.

(71) Khan, M.; Luque, R.; Akhtar, S.; Shaheen, A.; Mehmood, A.; Idress, S.; Buzdar, S.; ur Rehman, A. Design of Anion Exchange Membranes and Electrodialysis Studies for Water Desalination. *Materials* **2016**, *9* (5), 365.

(72) Chakrabarty, T.; Singh, A. K.; Shahi, V. K. Zwitterionic silica copolymer based crosslinked organic-inorganic hybrid polymer electrolyte membranes for fuel cell applications. *RSC Adv.* **2012**, *2* (5), 1949−1961.

(73) Hayat, M.; Manzoor, S.; Raza, H.; Khan, M. I.; Shanableh, A.; Sajid, M.; Almutairi, T. M.; Luque, R. Molecularly imprinted ormosil as a sorbent for targeted dispersive solid phase micro extraction of pyriproxyfen from strawberry samples. *Chemosphere* **2023**, *320*, 137835.

(74) Ho, Y. S.; McKay, G. Pseudo-second order model for sorption processes. *Process Biochemistry* **1999**, *34* (5), 451−465.

(75) Sahoo, T. R.; Prelot, B. Adsorption processes for the removal of contaminants from wastewater: the perspective role of nanomaterials and nanotechnology. In *Nanomaterials for the detection and removal of wastewater pollutants*; Bonelli, B., Freyria, F. S., Rossetti, I., Sethi, R., Eds; Elsevier, 2020; pp 161−222.

(76) Elzahar, M. M. H.; Bassyouni, M. Removal of direct dyes from wastewater using chitosan and polyacrylamide blends. *Sci. Reports* **2023**, *13* (1), 15750.

(77) Murcia-Salvador, A.; Pellicer, J. A.; Fortea, M. I.; Gómez-López, V. M.; Rodríguez-López, M. I.; Núñez-Delicado, E.; Gabaldón, J. A. Adsorption of Direct Blue 78 Using Chitosan and Cyclodextrins as Adsorbents. *Polymers* **2019**, *11* (6), 1003.

(78) Zheng, X.; Yu, N.; Wang, X.; Wang, Y.; Wang, L.; Li, X.; Hu, X. Adsorption Properties of Granular Activated Carbon-Supported Titanium Dioxide Particles for Dyes and Copper Ions. *Sci. Rep.* **2018**, *8* (1), 6463.

(79) Khan, M. I.; Shanableh, A.; Manzoor, S.; ur Rehman, A.; Shahida, S.; Ahmad, F. Application of United Arab Emirates Arecaceae leaves biochar for adsorptive removal of Rhodamine B from an aqueous solution. *Desal. Water Treat.* **2023**, *283*, 247−258.

(80) Nizam, N. U. M.; Hanafiah, M. M.; Mahmoudi, E.; Halim, A. A.; Mohammad, A. W. The removal of anionic and cationic dyes from an aqueous solution using biomass-based activated carbon. *Sci. Reports* **2021**, *11* (1), 8623.

(81) Khan, M. I.; Zafar, S.; Azhar, M. F.; Buzdar, A. R.; Hassan, W.; Aziz, A.; Khraisheh, M. Leaves powder of syzgium cumini as an adsorbent for removal of congo red dye from aqueous solution. *Fresenius Environ. Bull.* **2018**, *27* (5A), 3342−3350.